Journal of Applied Mechanics and Technical Physics, Vol. 43, No. 4, pp. 593–602, 2002

WATER INJECTION INTO A GEOTHERMAL RESERVOIR

V. Sh. Shagapov,[1] **U. R. Il'yasov,**[2] **and L. A. Nasyrova**[3]

UDC 532.546; 536.421

The previously obtained criterion which distinguishes water injection regimes accompanied by vaporization of injected water or vapor condensation is extended to the radially symmetric problem. The effects of cold liquid injection rate and the initial temperature, pressure, and capacity of a geothermal reservoir on hydrodynamic and temperature profiles are examined.

Introduction. Heat from an underground high-temperature reservoir which is a porous permeable rock is obtained as a heat carrier (usually hot water or vapor). A method for extracting this heat, especially in the case where the porous medium is initially saturated with vapor is the production of artificial circular systems by injecting water into heated permeable rock. Some aspects of this problem are considered in [1–7].

The goals of the present paper are as follows: analysis of the effect of parameters of a vapor-saturated porous medium and cold liquid injection rates on temperature and hydrodynamic fields; determination of conditions that allows differentiation between filtration regimes involving vaporization of the injected liquid and the regimes accompanied by vapor condensation; construction of analytical solutions for rather high injection rates, which are of greatest practical interest.

1. Constitutive Equations. To describe filtration processes and heat and mass transfer during water injection into a porous medium, we use the following assumptions. The temperatures of the porous medium and the saturating material (water or vapor) are identical. In addition, we assume that the skeleton of the porous medium is incompressible and immovable, and the porosity is constant.

Within the framework of the adopted assumptions, the conservation equation for the mass of water (vapor) is written as

$$\frac{\partial(m\rho_i)}{\partial t} + r^{-n}\,\frac{\partial}{\partial r}(r^n m\rho_i v_i) = 0,$$

where m is the porosity, ρ_i ($i = \text{liq}$ or vap) are the densities of the phases, v_i ($i = \text{liq}$ or vap) are the phase velocities, r is the coordinate, and t is time; the subscripts "liq," "vap," and "sk" correspond to the water, vapor, and porous skeleton, respectively

For water and vapor filtration, we use the Darcy law

$$mv_i = -\frac{k}{\mu_i}\,\frac{\partial p}{\partial r} \qquad (i = \text{liq, vap}),$$

where k and μ_i are the absolute permeability and dynamic viscosity of the phases.

The equation of heat inflow ignoring the barometric effect is written as

$$\rho c\,\frac{\partial T}{\partial t} + m\rho_i c_i v_i\,\frac{\partial T}{\partial r} = r^{-n}\,\frac{\partial}{\partial r}\Big(r^n\lambda\,\frac{\partial T}{\partial r}\Big),$$

$$\rho c = m\rho_i c_i + (1-m)\rho_{\rm sk}c_{\rm sk}, \qquad \lambda = m\lambda_i + (1-m)\lambda_{\rm sk} \qquad (i = \text{liq, vap}).$$

Here ρc is the specific volume heat of the system "porous medium–vapor (water)," c_i and λ_i are the specific heat and thermal conductivity of the phases, and λ is the thermal conductivity of the system "porous medium–vapor

[1]Institute of Mechanics, Ufa Scientific Center, Russian Academy of Sciences, Ufa 450025. [2]Sterlitamak State Pedagogical Institute, Sterlitamak 450103. [3]Ufa Technological Institute of Service, Ufa 450000. Translated from Prikladnaya Mekhanika i Tekhnicheskaya Fizika, Vol. 43, No. 4, pp. 127–138, July–August, 2002. Original article submitted April 3, 2001; revision submitted February 26, 2002.

(water)." Because the parameters of the skeleton of the porous medium make a major contribution to the values of ρc and λ, we consider them constant ($\rho c = \text{const}$ and $\lambda = \text{const}$) over the entire filtration zone (vapor and water filtration zone).

For the vapor, we use the Clapeyron–Mendeleev equation, and the water is considered incompressible:

$$\rho_{\text{vap}} = p/(R_{\text{vap}}T), \qquad \rho_{\text{liq}} = \rho_{\text{liq},0}.$$

Here p and T are the pressure and temperature and R_{vap} is the gas constant; the subscript 0 corresponds to parameters of the initial (undisturbed) state of the porous medium.

The above equations must be supplemented by the relations on the phase-transition surface ($r = r_{(s)}$) that follow from the law of conservation of mass and the heat-balance condition:

$$m\rho_{\text{liq}}(v_{\text{liq}} - \dot r_{(s)}) = m\rho_{\text{vap}}(v_{\text{vap}} - \dot r_{(s)}), \quad \Big(\lambda \frac{\partial T}{\partial r}\Big)^+ - \Big(\lambda \frac{\partial T}{\partial r}\Big)^- = m\rho_{\text{liq}} l (v_{\text{liq}} - \dot r_{(s)}), \quad \dot r_{(s)} = \frac{dr_{(s)}}{dt}. \tag{1.1}$$

Here l is the specific heat of the phase transition. The subscript (s) corresponds to parameters on the phase-transition boundary. On this boundary, the temperature and pressure are considered continuous:

$$T^- = T^+ = T_{(s)}, \qquad p^- = p^+ = p_{(s)}.$$

In addition, on the phase-transition surface, the temperature $T_{(s)}$ and the pressure $p_{(s)}$ are related by the equation

$$T_{(s)} = T_* \ln^{-1}(p_*/p_{(s)}),$$

where T_* and p_* are empirical parameters determined from table data.

Along with the phase-transition front, we introduce a labelled boundary ($r = r_{(m)}$) of the injected system, which is determined from the condition of equality of the rates of motion of water (vapor) and this boundary ($v = \dot r_{(m)}$). In the regime in which vapor condensation occurs on the phase-transition boundary, the labelled boundary $r_{(m)}$ is behind the phase-transition front (i.e., in the water filtration region), and in the regime involving vaporization of injected water, it is ahead of the phase-transition front (i.e., in the vapor filtration region). Thus, there is an intermediate zone between the phase-transition front and the labelled boundary. In the first filtration regime, condensed vapor is present in this zone, and in the second regime, vaporized water is present there. The labelled boundary for the two regimes is determined from the condition $v_{\text{liq}} = \dot r_{(m)}$ or $v_{\text{vap}} = \dot r_{(m)}$ ($r = r_{(m)}$).

Let us consider the one-dimensional [flat ($n = 0$) and axisymmetric ($n = 1$)] problems of injection of water having temperature T_e into the porous medium saturated with vapor. We assume that in the initial state, the geothermal reservoir at temperature T_0 is completely saturated with vapor and is under pressure p_0. Injection occurs at constant pressure p_e on the boundary ($n = 0$) or constant volume flow rate q ($n = 1$). With allowance for the assumptions made above, the initial and boundary conditions are written as

$$\begin{aligned} &n = 0\colon \quad p = p_0, \quad T = T_0 \quad (r > 0,\ t = 0), \quad p = p_e, \quad T = T_e \quad (r = 0,\ t > 0), \\ &n = 1\colon \quad p = p_0, \quad T = T_0 \quad (r > 0,\ t = 0), \quad -2\pi r\Big(\frac{k}{\mu_{\text{liq}}}\frac{\partial p}{\partial r}\Big) = q, \quad T = T_e \quad (r \to 0,\ t > 0). \end{aligned} \tag{1.2}$$

We introduce the dimensionless parameter γ, which is the ratio of the total rate of vaporization on the phase-transition boundary to the total amount of injected water:

$$n = 0\colon \quad \gamma = (v_{\text{liq}} - \dot r_{(s)})/v_{\text{liq}}, \qquad n = 1\colon \quad \gamma = 2\pi r_{(s)} m (v_{\text{liq}} - \dot r_{(s)})/q.$$

Within the framework of the system considered, both problems are self-similar.

We introduce dimensionless pressure, temperature, density, and a self-similar variable:

$$P = \frac{p}{p_0}, \quad \Theta = \frac{T}{T_0}, \quad \tilde\rho = \frac{\rho_{\text{vap}}}{\rho_{\text{vap},0}} = \frac{P}{\Theta}, \quad \xi = \frac{r}{2\sqrt{at}} \quad \Big(a = \frac{\lambda}{\rho c}\Big).$$

Then, the heat- and piezoconduction equations can be written as

$$\xi^{-n}\frac{d}{d\xi}\Big(\xi^n \frac{dP}{d\xi}\Big) = 0, \quad \xi^{-n}\frac{d}{d\xi}\Big(\xi^n \frac{d\Theta}{d\xi}\Big) = -2\xi\frac{d\Theta}{d\xi} - \text{Pe}_{\text{liq}}\frac{dP}{d\xi}\frac{d\Theta}{d\xi} \quad (0 < \xi < \xi_{(s)}); \tag{1.3}$$

$$\begin{aligned} &\eta_{\text{vap}}\xi^{-n}\frac{d}{d\xi}\Big(\xi^n\tilde\rho\frac{dP}{d\xi}\Big) = -2\xi\frac{d}{d\xi}\tilde\rho, \\ &\xi^{-n}\frac{d}{d\xi}\Big(\xi^n \frac{d\Theta}{d\xi}\Big) = -2\xi\frac{d\Theta}{d\xi} - \text{Pe}_{\text{vap}}\frac{dP}{d\xi}\frac{d\Theta}{d\xi} \quad (\xi_{(s)} < \xi < \infty), \end{aligned} \tag{1.4}$$

where Pe_i is the Peclet number. In this case, on the phase-transition boundary ($\xi = \xi_{(s)}$), we have

$$\eta_{\mathrm{vap}}\Big(\tilde\rho_{(s)}\Big(\frac{dP}{d\xi}\Big)^{+} - \tilde\mu\Big(\frac{dP}{d\xi}\Big)^{-}\Big) = 2(1-\tilde\rho_{(s)})\xi_{(s)}, \qquad \Big(\frac{d\Theta}{d\xi}\Big)^{+} - \Big(\frac{d\Theta}{d\xi}\Big)^{-} = -\frac{m\tilde\rho_{\mathrm{liq}}}{\mathrm{Ja}}\Big(\eta_{\mathrm{liq}}\Big(\frac{dP}{d\xi}\Big)^{-} + 2\xi_{(s)}\Big); \tag{1.5}$$

$$\Theta_{(s)} = \Theta_* \ln^{-1}(P_*/P_{(s)}), \tag{1.6}$$

where Ja is the Jacobi number.

In Eqs. (1.3)–(1.6), the dimensionless coefficients are written as

$$\mathrm{Pe}_i = \frac{\rho_i c_i}{\lambda}\,\frac{kp_0}{\mu_i} \quad (i = \mathrm{liq},\ \mathrm{vap}), \qquad \eta_i = \frac{æ_i}{a}, \quad æ_i = \frac{p_0 k}{m\mu_i} \quad (i = \mathrm{liq},\ \mathrm{vap}),$$

$$P_* = \frac{p_*}{p_0}, \quad \Theta_* = \frac{T_*}{T_0}, \quad \tilde\rho_{(s)} = \frac{\rho_{\mathrm{vap}(s)}}{\rho_{\mathrm{liq}}}, \quad \tilde\rho_{\mathrm{liq}} = \frac{\rho_{\mathrm{liq}}}{\rho}, \quad \tilde\mu = \frac{\mu_{\mathrm{vap}}}{\mu_{\mathrm{liq}}}, \quad \mathrm{Ja} = \frac{cT_0}{l}.$$

From the initial and boundary conditions (1.2) it follows that

$$n = 0: \qquad P = P_e,\ \Theta = \Theta_e \text{ for } \xi = 0, \quad P = 1,\ \Theta = 1 \text{ for } \xi = \infty,$$

$$n = 1: \qquad \xi\Big(\frac{dP}{d\xi}\Big)_{\xi} = -\tilde q,\ \Theta = \Theta_e \text{ as } \xi \to 0 \ \Big(\tilde q = \frac{\mu_{\mathrm{liq}} q}{2\pi k p_0}\Big), \quad P = 1,\ \Theta = 1 \text{ for } \xi = \infty. \tag{1.7}$$

In this case, the equation for the self-similar coordinate $\xi_{(m)} = r_{(m)}/(2\sqrt{at}\,)$ of the labelled boundary can be written as

$$\eta_i\Big(\frac{dP}{d\xi}\Big) = -2\xi_{(m)} \qquad (\xi = \xi_{(m)}), \tag{1.8}$$

where $i = \mathrm{liq}$ or vap if the labelled boundary is in the regions of filtration of vapor or water, respectively.

Unlike in [7], in the present paper, the compressibility of the liquid was ignored. An analysis of the solutions shows that for the plane problem ($n = 0$), this approximation is valid for rather low pressure drops: $\Delta p \ll p_*$ ($\Delta p = p_e - p_0$ and $p_* = 2\rho_{\mathrm{liq}}C_{\mathrm{liq}}^2$, where C_{liq} is the velocity of sound in the liquid), and in the axisymmetric problem, it is valid for low rates of liquid injection: $q \ll q_*$ ($q_* = 4\pi k\rho_{\mathrm{liq}}C_{\mathrm{liq}}^2/\mu_{\mathrm{liq}}$). In particular, for cold water injection ($T_e = 300$ K and $C_{\mathrm{liq}} = 1500$ m/sec) into a reservoir with permeability $k = 10^{-12}$ m^2, the critical pressure drop and injection rate are equal to $p_* = 4\cdot 10^9$ Pa and $q_* = 25$ m^3/(m $\cdot$ sec), respectively. Therefore, the adopted model with an incompressible liquid is valid over the entire range of pressure drops Δp and injection rates q of practical interest.

The adopted model with constant porosity assumes that the skeleton is cemented rock. Because the compressibility of rock is well below the compressibility of water, this assumption practically does not narrow the region of applicability of the results.

2. Analysis of the Solutions. Equations (1.3), describing waters filtration, can be integrated. Then, for the pressure and temperature distributions in the water filtration region, we have

$$n = 0: \qquad P = P_e + (P_{(s)} - P_e)\frac{\xi}{\xi_{(s)}},$$

$$\Theta = \Theta_e + (\Theta_{(s)} - \Theta_e)\int_0^{\xi} \exp(\beta\xi - \xi^2)\,d\xi \Big/ \int_0^{\xi_{(s)}} \exp(\beta\xi - \xi^2)\,d\xi \tag{2.1}$$

$$[\beta = \mathrm{Pe}_{\mathrm{liq}}(P_e - P_{(s)})\xi_{(s)}^{-1}];$$

$$n = 1: \qquad P = P_{(s)} + \tilde q \ln\frac{\xi_{(s)}}{\xi}, \quad \Theta = \Theta_e + (\Theta_{(s)} - \Theta_e)\int_0^{\xi} \xi^{\varphi}\exp(-\xi^2)\,d\xi \Big/ \int_0^{\xi_{(s)}} \xi^{\varphi}\exp(-\xi^2)\,d\xi$$

$$[\varphi = \rho_{\mathrm{liq}} c_{\mathrm{liq}} q/(2\pi\lambda) - 1]. \tag{2.2}$$

In the case where the labelled boundary is in the water filtration region (filtration is accompanied by vapor condensation), for its self-similar coordinate based on (1.8), using (2.1) and (2.2), we obtain

$$n = 0: \quad \xi_{(m)} = (P_e - P_{(s)})\eta_{\rm liq}/(2\xi_{(s)}), \qquad n = 1: \quad \xi_{(m)} = \tilde{q}\eta_{\rm liq}/2.$$

For the vaporized fraction of injected water, we can write

$$n = 0: \quad \gamma = 1 - \xi^2_{(s)}/[(P_e - P_{(s)})\eta_{\rm liq}], \qquad n = 1: \quad \gamma = 1 - \xi^2_{(s)}/(\tilde{q}\eta_{\rm liq}).$$

From solutions (2.1) and (2.2) it follows that in the water filtration region, the temperature field is determined primarily by convective heat transfer at rather high rate of water injection when the condition $P_e - P_{(s)} \gg \mathrm{Pe}_{\rm liq}^{-1}$ is satisfied for the plane problem ($n = 0$) and the condition $q \gg 2\pi\lambda/(\rho_{\rm liq}c_{\rm liq})$ is satisfied for the axisymmetric problem ($n = 1$).

Substituting solutions (2.1) and (2.2) into Eqs. (1.5), which follow from the conditions on the phase-transition boundary ($\xi = \xi_{(s)}$), we obtain

$$n = 0: \qquad \Big(\frac{dP}{d\xi}\Big)^+ = -\frac{\tilde{\mu}(P_{(s)} - P_e)}{\tilde{\rho}_{(s)}\xi_{(s)}} + 2\,\frac{(\tilde{\rho}^{-1}_{(s)} - 1)\xi_{(s)}}{\eta_{\rm vap}},$$

$$\Big(\frac{d\Theta}{d\xi}\Big)^+ = (\Theta_{(s)} - \Theta_e)\exp\,(\beta\xi_{(s)} - \xi^2_{(s)}) \Big/ \int\limits_0^{\xi_{(s)}} \exp\,(\beta\xi - \xi^2)\,d\xi + \frac{m\tilde{\rho}_{\rm liq}}{\rm Ja}\Big(\frac{\eta_{\rm liq}(P_{(s)} - P_e)}{\xi_{(s)}} - 2\xi_{(s)}\Big); \quad (2.3)$$

$$n = 1: \qquad \Big(\frac{dP}{d\xi}\Big)^+ = -\frac{\tilde{\mu}\tilde{q}}{\tilde{\rho}_{(s)}\xi_{(s)}} + 2\,\frac{(\tilde{\rho}^{-1}_{(s)} - 1)\xi_{(s)}}{\eta_{\rm vap}},$$

$$\Big(\frac{d\Theta}{d\xi}\Big)^+ = (\Theta_{(s)} - \Theta_e)\xi^{\varphi}_{(s)}\exp\,(-\xi^2_{(s)}) \Big/ \int\limits_0^{\xi_{(s)}} \xi^{\varphi}\exp\,(-\xi^2)\,d\xi + \frac{m\tilde{\rho}_{\rm liq}}{\rm Ja}\Big(\frac{\eta_{\rm liq}\tilde{q}}{\xi_{(s)}} - 2\xi_{(s)}\Big). \quad (2.4)$$

In the general formulation, the examined self-similar problem for the system of ordinary differential equations (1.3) and (1.4) is a boundary-value problem with the conditions at $\xi = 0$ and $\xi = \infty$ corresponding to the boundary and initial conditions (1.7). In addition, in the problem there is an intermediate unknown boundary ($\xi = \xi_{(s)}$), which corresponds to the phase-transition front, on which the joining conditions (1.5) and the pressure and temperature continuity conditions ($P^+ = P^- = P_{(s)}$ and $\Theta^+ = \Theta^- = \Theta_{(s)}$) should be satisfied [$\Theta_{(s)} = \Theta_* \ln^{-1}(P_*/P_{(s)})$]. In the water filtration region, system (1.3) has the analytical solutions (2.1) and (2.2). Using these solutions and the joining conditions (1.5) and (1.6) in the vapor filtration region for Eqs. (1.4), the boundary-value problem is solved numerically by the point matching method. In this case, each point matching is a Cauchy problem. For specified values of the self-similar coordinate of the phase-transition boundary $\xi_{(s)} = \xi^*_{(s)}$, the initial data are the values of the pressure $P(\xi^*_{(s)})$, the temperature $\Theta(\xi^*_{(s)})$, and the derivatives of the pressure $P'(\xi^*_{(s)})$ and temperature $\Theta'(\xi^*_{(s)})$, determined from solutions (2.1) and (2.2) and relations (1.6), (2.3), and (2.4). Selection of values of $\xi^*_{(s)}$ continues until the pressure and temperature at infinity ($\xi = \infty$) satisfy the corresponding second boundary conditions in (1.7) with specified accuracy.

In the case where in the heat-conduction equation (1.4) the term due to convection ($\mathrm{Pe}_{\rm vap} \ll 1$) can be ignored, the solution of system (1.4) can be written as

$$P = 1 + \Big(P_{(s)} - 1 + \frac{\Theta_{(s)} - 1}{\tilde{\eta}_{\rm vap} - 1}\Big)\int\limits_{\xi}^{\infty} \xi^{-n}\exp\Big(-\frac{\xi^2}{\tilde{\eta}_{\rm vap}}\Big)d\xi \Big/ \int\limits_{\xi_{(s)}}^{\infty} \xi^{-n}\exp\Big(-\frac{\xi^2}{\tilde{\eta}_{\rm vap}}\Big)d\xi$$

$$- \frac{\Theta_{(s)} - 1}{\tilde{\eta}_{\rm vap} - 1}\int\limits_{\xi}^{\infty} \xi^{-n}\exp\,(-\xi^2)\,d\xi \Big/ \int\limits_{\xi_{(s)}}^{\infty} \xi^{-n}\exp\,(-\xi^2)\,d\xi, \quad (2.5)$$

$$\Theta = 1 + (\Theta_{(s)} - 1)\int\limits_{\xi}^{\infty} \xi^{-n}\exp\,(-\xi^2)\,d\xi \Big/ \int\limits_{\xi_{(s)}}^{\infty} \xi^{-n}\exp\,(-\xi^2)\,d\xi \qquad (\tilde{\eta}_{\rm vap} = \eta_{\rm vap}\tilde{P}).$$

Substituting these solutions into conditions (2.3) and (2.4), we obtain

$$n = 0: \quad \Big(P_{(s)} - 1 + \frac{\Theta_{(s)} - 1}{\tilde{\eta}_{\rm vap} - 1}\Big)\exp\Big(-\frac{\xi_{(s)}^2}{\tilde{\eta}_{\rm vap}}\Big)\Big/\int\limits_{\xi_{(s)}}^{\infty} \exp\Big(-\frac{\xi^2}{\tilde{\eta}_{\rm vap}}\Big)d\xi$$

$$- \frac{\Theta_{(s)} - 1}{\tilde{\eta}_{\rm vap} - 1}\exp(-\xi_{(s)}^2)\Big/\int\limits_{\xi_{(s)}}^{\infty} \exp(-\xi^2)\,d\xi - \frac{\tilde{\mu}(P_{(s)} - P_e)}{\tilde{\rho}_{(s)}\xi_{(s)}} + 2\,\frac{\xi_{(s)}}{\eta_{\rm vap}}\Big(\frac{1}{\tilde{\rho}_{(s)}} - 1\Big) = 0,$$

$$(\Theta_{(s)} - 1)\Big/\int\limits_{\xi_{(s)}}^{\infty} \exp(-\xi^2)\,d\xi + (\Theta_{(s)} - \Theta)\exp(\beta\xi_{(s)})\Big/\int\limits_{\xi_{(s)}}^{\infty} \exp(\beta\xi - \xi^2)\,d\xi$$

$$+ m\tilde{\rho}_{\rm liq}\exp(\xi_{(s)}^2)[\eta_{\rm liq}(P_{(s)} - P_e)/\xi_{(s)} - 2\xi_{(s)}]/{\rm Ja} = 0; \tag{2.6}$$

$$n = 1: \quad \Big(P_{(s)} - 1 + \frac{\Theta_{(s)} - 1}{\tilde{\eta}_{\rm vap} - 1}\Big)\exp\Big(-\frac{\xi_{(s)}^2}{\tilde{\eta}_{\rm vap}}\Big)\Big/\int\limits_{\xi_{(s)}}^{\infty} \xi^{-1}\exp\Big(-\frac{\xi^2}{\tilde{\eta}_{\rm vap}}\Big)d\xi$$

$$- \frac{\Theta_{(s)} - 1}{\tilde{\eta}_{\rm vap} - 1}\exp(-\xi_{(s)}^2)\Big/\int\limits_{\xi_{(s)}}^{\infty} \xi^{-1}\exp(-\xi^2)\,d\xi - \frac{\tilde{\mu}\tilde{q}}{\tilde{\rho}_{(s)}} + 2\,\frac{\xi_{(s)}^2}{\eta_{\rm vap}}\Big(\frac{1}{\tilde{\rho}_{(s)}} - 1\Big) = 0,$$

$$(\Theta_{(s)} - 1)\Big/\int\limits_{\xi_{(s)}}^{\infty} \xi^{-1}\exp(-\xi^2)\,d\xi + (\Theta_{(s)} - \Theta_e)\xi_{(s)}^{\varphi+1}\Big/\int\limits_{0}^{\xi_{(s)}} \xi^{\varphi}\exp(-\xi^2)\,d\xi + m\tilde{\rho}_{\rm liq}\exp(\xi_{(s)}^2)(\eta_{\rm liq}\tilde{q} - 2\xi_{(s)}^2)/{\rm Ja} = 0.$$

Here $\tilde{\eta}_{\rm vap} = \eta_{\rm vap}\tilde{P}$ is the dimensionless piezocnductivity for the linearized equation of filtration in the region of vapor motion. In the calculations, we used two limiting values $\tilde{P}$: $\tilde{P} = 1$ and $\tilde{P} = P_{(s)}$, and for $\tilde{P} = 1$, linearization is performed near the initial value of the pressure in the porous medium ($p = p_0$), and for $\tilde{P} = P_{(s)}$, it is performed near the value of the pressure on the phase-transition boundary. Numerical analysis shows that the best fit of the linearized analytical solutions to the solution of the complete system of nonlinear filtration and heat-transfer equations is obtained for $\tilde{P} = P_{(s)}$. It should be noted that for $n = 0$ and in the absence of convective heat transfer in the water filtration region, solutions (2.1) and (2.5) coincide with the solution given in [7]. If filtration is accompanied by water vaporization, for the labelled boundary in the vapor filtration region, we use solution (2.5) for the pressure distribution. As a result, for (1.8) we obtain the equation for the self-similar coordinate $\xi_{(m)}$:

$$\Big(P_{(s)} - 1 + \frac{\Theta_{(s)} - 1}{\tilde{\eta}_{\rm vap} - 1}\Big)\xi_{(m)}^{-n}\exp\Big(-\frac{\xi_{(m)}^2}{\tilde{\eta}_{\rm vap}}\Big)\Big/\int\limits_{\xi_{(s)}}^{\infty} \xi^{-n}\exp\Big(-\frac{\xi^2}{\tilde{\eta}_{\rm vap}}\Big)\,d\xi$$

$$- \frac{\Theta_{(s)} - 1}{\tilde{\eta}_{\rm vap} - 1}\,\xi_{(m)}^{-n}\exp(-\xi_{(m)}^2)\Big/\int\limits_{\xi_{(s)}}^{\infty} \xi^{-n}\exp(-\xi^2)\,d\xi = \frac{2\xi_{(m)}}{\eta_{\rm vap}}. \tag{2.7}$$

Figure 1 shows pressure and temperature distributions for slow rate ($q = 10^{-6}$ m^2/sec) of water injection at temperature $T_e = 280$ K. Curves 1 and 2 correspond to the initial temperatures of the porous medium $T_0 = 373$ and 393 K. For the remaining parameters determining the state and the properties of the system, the following values are used: $p_0 = 10^5$ Pa, $k = 10^{-15}$ m^2, $R_{\rm vap} = 461$ J$\cdot$kg/K, $\rho_{\rm liq,0} = 1000$ kg/m^3, $\rho_{\rm sk} = 2\cdot 10^3$ kg/m^3, $\lambda_{\rm liq} = 0.58$ W/(m$\cdot$K), $\lambda_{\rm sk} = 2$ W/(m$\cdot$K), $\lambda_{\rm vap} = 0.02$ W/(m$\cdot$K), $c_{\rm liq} = 4.2\cdot 10^3$ J/(kg$\cdot$K), $c_{\rm sk} = 0.9\cdot 10^3$ J/(kg$\cdot$K), $p_* = 27{,}542$ MPa, $T_* = 4616$ K, $l = 1.85\cdot 10^6$ J/kg, $\mu_{\rm liq} = 1.1\cdot 10^{-3}$ Pa$\cdot$sec, and $\mu_{\rm vap} = 1.21\cdot 10^{-5}$ Pa$\cdot$sec. In Fig. 1 it is evident that in the case where in the initial state, the vapor in the porous medium is near the saturation point (curve 1), the pressure distribution is nonmonotonic: the pressure on the phase-transition boundary is below the initial pressure in the porous medium ($P_{(s)} < 1$). The dashed curves in Fig. 1 correspond to the dimensionless saturation temperature $\Theta_{(s)}(P)$.

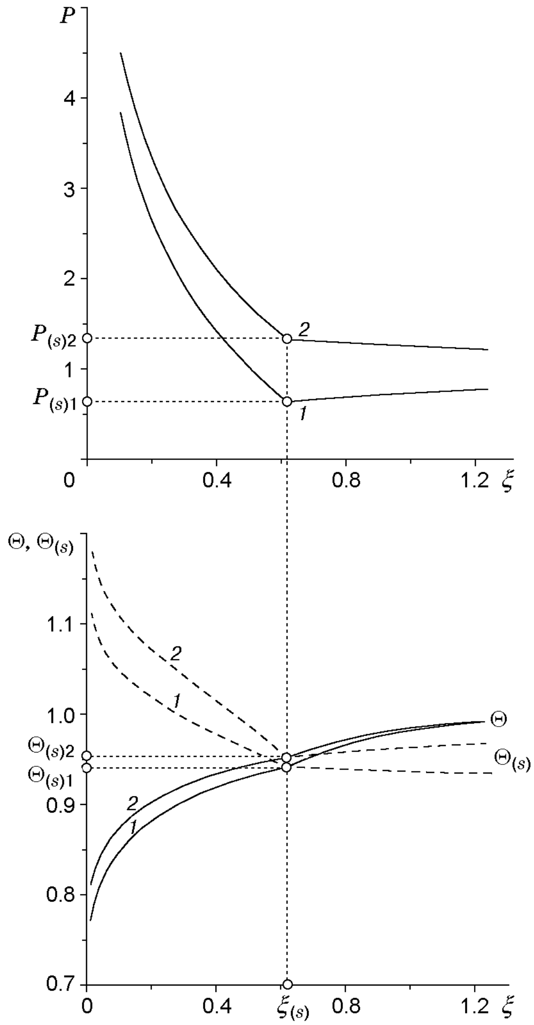

Fig. 1

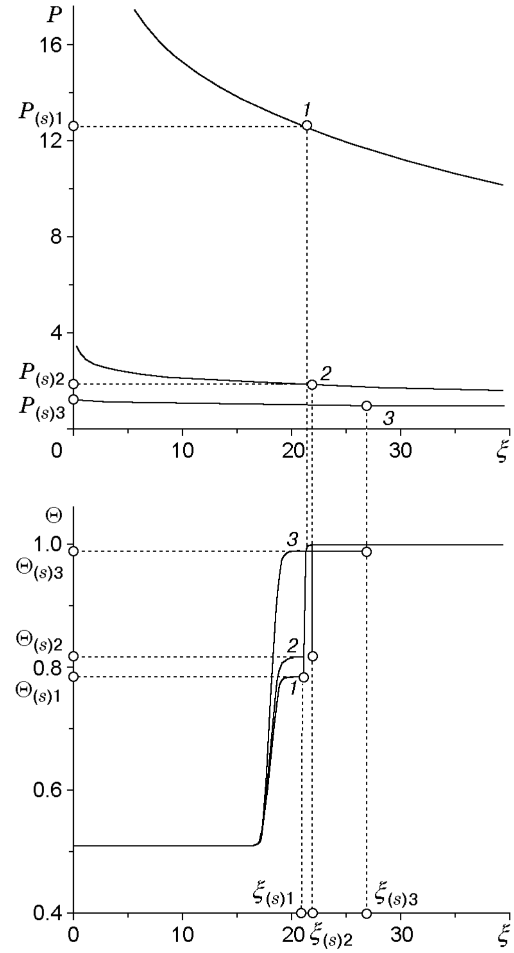

Fig. 2

Fig. 1. Pressure and temperature distribution for initial temperatures of the porous medium $T_0 = 373$ (1) and 393 K.

Fig. 2. Pressure and temperature distribution for initial pressures of the porous medium $p_0 = 10^5$ (1), 10^6 (2), and 10^7 Pa (3).

We obtain a condition for occurrence of a pressure "well" (Fig. 1) in the general case. From boundary conditions (1.1) it follows that vapor condensation and formation of a pressure "well" near the phase-transition boundary occur for $\rho_{\rm liq} l m v_{\rm liq} \ll \lambda(\partial T/\partial r)^-$.

Using the estimates

$$mv_{\rm liq} = -\frac{k}{\mu_{\rm liq}}\Big(\frac{\partial p}{\partial r}\Big)^- \approx \frac{k}{\mu_{\rm liq}}\,\frac{\Delta p}{r_{(s)}}, \qquad \Big(\frac{\partial T}{\partial r}\Big)^- \approx \frac{\Delta T}{r_{(s)}} \quad (\Delta T = T_0 - T_e,\ \Delta p = p_e - p_0)$$

for the plane problem ($n = 0$) and the estimates

$$mv_{\rm liq} = \frac{q}{2\pi r_{(s)}}, \qquad \Big(\frac{\partial T}{\partial r}\Big)^- = \frac{\Delta T}{r_{(s)}}$$

for the axisymmetric problem ($n = 1$), we find that filtration accompanied by vapor condensation is ensured by the conditions

$$n = 0:\quad \Delta T \gg k\rho_{\rm liq} l\Delta p/(\mu_{\rm liq}\lambda), \qquad n = 1:\quad \Delta T \gg \rho_{\rm liq} lq/(2\pi\lambda). \tag{2.8}$$

The first condition ($n = 0$) coincides with the condition given in [7]. Although these conditions are in good agreement with results of numerical analysis, they are valid in practice only for a narrow range of values ΔT, Δp, and q and low

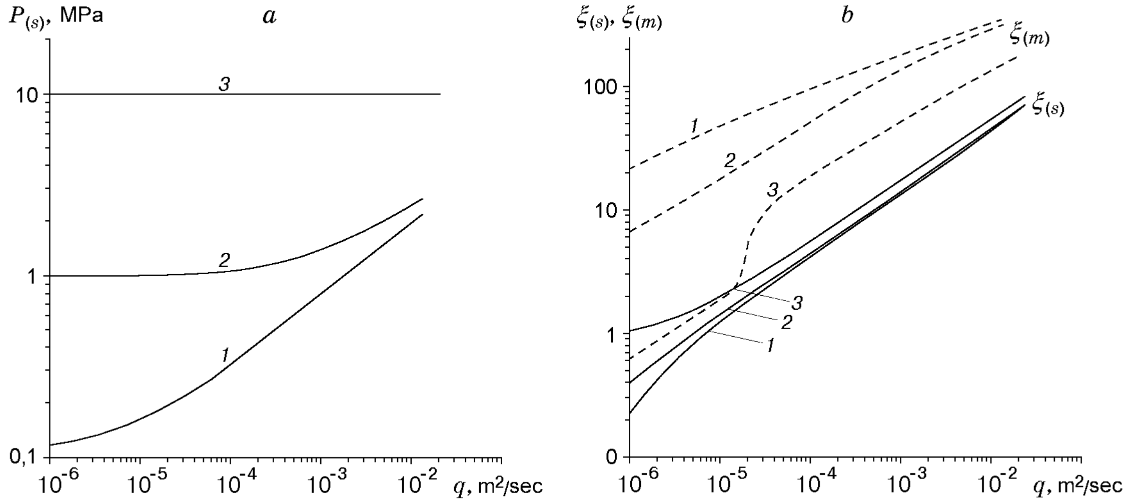

Fig. 3. Pressure $P_{(s)}$ on the phase-transition boundary (a), and the position of this boundary $\xi_{(s)}$ and the labelled boundary $\xi_{(m)}$ (b) versus the flow rate of injected water q for $p_0 = 10^5$ (1), 10^6 (2), and 10^7 Pa (3).

permeability k. For the axisymmetric problem, condition (2.8) can be satisfied only for low rates of water injection. In particular, for real values of the temperature ($\Delta T = 1$–10^2 K) and pressure drop ($\Delta p = 0.1$–10 MPa), the first condition in (2.8) can be satisfied for $k \ll 10^{-16}$ m^2. In this case, because of capillary effects, the filtration pattern is obviously different. We estimate the characteristic capillary pressure Δp_σ using the expression $\Delta p_\sigma = \sigma/d$ (σ is the surface tension and $d \approx \sqrt{k/m}$ is the linear pore size). For $k \ll 10^{-16}$ m^2 for water ($\sigma = 0.05$ kg/sec^2) with $m = 0.1$, we obtain $\Delta p_\sigma \gg 1$ MPa. It should be noted that the filtration regime with a pressure "well" and an intermediate two-phase zone considered in [6] for $k = 10^{-17}$ m^2 is difficult to attain.

For various initial pressures in the porous medium, Fig. 2 gives temperature and pressure distributions in self-similar variables for the axisymmetric problem ($n = 1$) of water injection at temperature $T_e = 300$ K and volume flow rate $q = 2\cdot 10^{-3}$ m^2/sec into a porous medium with temperature $T_0 = 590$ K, porosity $m = 0.2$, and permeability $k = 10^{-12}$ m^2. Curves 1–3 correspond to initial vapor pressures in the porous medium $p_0 = 10^5$, 10^6, and 10^7 Pa, respectively. In this case, $\xi_{(m)} = 210.6$, 177.4, and 37.4 and $\gamma = 0.23$, 0.15, and 0.14, respectively. In Fig. 2 one can see three characteristic regions in each of which the temperature is nearly constant. For higher values of the initial pressure p_0 of the porous medium and injection rate q of the liquid, the stepped temperature distribution becomes more pronounced. In this case, in the regions near and away from the injection site, the temperature is equal to the injected water temperature and the initial temperature of the porous medium, respectively. In the intermediate zone which is in the water filtration region behind the phase-transition boundary, the temperature and the extent of this zone depend on the initial pressure in the porous medium. With increase in the initial pressure p_0, the extent and temperature of the intermediate zone increase. Therefore, at low initial pressures of the porous medium, the underground heat is expended primarily in vaporization of the injected liquid, and at high pressures, it is expended in heating of the liquid.

Figure 3 shows pressure curves on the phase-transition boundary $P_{(s)}$ and the self-similar coordinate of the boundary $\xi_{(s)}$, and the self-similar coordinate of the labelled boundary $\xi_{(m)}$ versus the flow rate of injected water. Curves 1–3 correspond to values $p_0 = 10^5$, 10^6, and 10^7 Pa, respectively.

3. Solution with Temperature Jumps. We consider the injection regime in which heat transfer in the liquid filtration region is determined primarily by the convective mechanism. In this case, as follows from an analysis of Figs. 2 and 3, the temperature distribution is close to the stepped one with two jumps. The first temperature jump is observed in the water filtration region, and the second near the phase-transition boundary. Thus, the temperature field in the filtration zone is actually determined by three temperature values [T_0, $T_{(s)}(p_{(s)})$, and T_e], and, hence, it is possible to construct an approximate solution with temperature jumps.

Let us write the heat-balance conditions on the boundaries of the two temperature jumps. For the first jump in the water filtration region ($r = r_{(T)}$), we have

$$v_{\text{liq}} - \dot r_{(T)} = \rho_{(s)}(1-m)c_{\text{sk}}(T_{(s)} - T_e)\dot r_{(T)}/[m\rho_{\text{liq}}c_{\text{liq}}(T_{(s)} - T_e)]. \tag{3.1}$$

For the second jump, whose position coincides with the phase-transition boundary ($r = r_{(s)}$), we can write

$$\rho_{\text{liq}}(v_{\text{liq}} - \dot r_{(s)}) = \rho_{(s)}(1-m)c_{\text{liq}}(T_0 - T_{(s)})\dot r_{(s)}/l', \qquad l' = l + c_{\text{vap}}(T_0 - T_{(s)}). \tag{3.2}$$

In addition, on this boundary we write the mass-balance condition

$$m\rho_{\text{liq}}(v_{\text{liq}} - \dot r_{(s)}) = m\rho_{\text{vap}}(v_{\text{vap}} - \dot r_{(s)}). \tag{3.3}$$

For the zone of water and vapor filtration, the piezoconduction equations are written as

$$r^{-n}\frac{\partial}{\partial r}\Big(r^n\frac{\partial p}{\partial r}\Big) = 0 \quad (0 < r < r_{(s)}), \qquad \frac{\partial p}{\partial t} = r^{-n}\frac{\partial}{\partial r}\Big(æ_{\text{vap}}r^n\frac{p}{p_0}\frac{\partial p}{\partial r}\Big) \quad (r_{(s)} < r < \infty). \tag{3.4}$$

We introduce the self-similar variable $\zeta = r/(2\sqrt{æ_{\text{liq}}t}\,)$. Then, conditions (3.1)–(3.3) can be written as

$$\frac{dP}{d\zeta} = -2(\text{Ja}_{(T)} + 1)\zeta_{(T)} \qquad (\zeta = \zeta_{(T)}); \tag{3.5}$$

$$\Big(\frac{dP}{d\zeta}\Big)^- = -2(\text{Ja}_{(s)} + 1)\zeta_{(s)}, \quad \tilde\rho_{(s)}\Big(\frac{dP}{d\zeta}\Big)^+ - \tilde\mu\Big(\frac{dP}{d\zeta}\Big)^- = 2\tilde\mu(1 - \tilde\rho_{(s)})\zeta_{(s)} \quad (\zeta = \zeta_{(s)}); \tag{3.6}$$

$$\text{Ja}_{(T)} = \frac{1-m}{m}\frac{\rho_{\text{sk}}}{\rho_{\text{liq}}}\frac{c_{\text{sk}}}{c_{\text{liq}}}, \qquad \text{Ja}_{(s)} = \frac{1-m}{m}\frac{\rho_{\text{sk}}}{\rho_{\text{liq}}}\frac{c_{\text{sk}}}{l'}(T_0 - T_{(s)}). \tag{3.7}$$

The solution of Eq. (3.4) subject to the initial and boundary conditions (1.2) can be written as

$$0 < \zeta < \zeta_{(s)}\colon \quad P = P_e + (P_{(s)} - P_e)\zeta/\zeta_{(s)} \quad (n = 0), \quad P = P_{(s)} + \tilde q\ln(\zeta_{(s)}/\zeta) \quad (n = 1); \tag{3.8}$$

$$\zeta_{(s)} < \zeta < \infty\colon \quad P = 1 + (P_{(s)} - 1)\int_\zeta^\infty \zeta^{-n}\exp\Big(-\frac{\zeta^2}{\tilde\eta}\Big)d\zeta \Big/ \int_{\zeta_{(s)}}^\infty \zeta^{-n}\exp\Big(-\frac{\zeta^2}{\tilde\eta}\Big)d\zeta, \tag{3.9}$$

where $\tilde q = q\mu_{\text{liq}}/(2\pi k p_0)$ and $\tilde\eta = æ_{\text{vap}}\tilde P/æ_{\text{liq}}$. In this case,

$$\Theta = \Theta_e \quad (0 < \zeta < \zeta_{(T)}), \qquad \Theta = \Theta_{(s)} \quad (\zeta_{(T)} < \zeta < \zeta_{(s)}), \qquad \Theta = 1 \quad (\zeta_{(s)} < \zeta < \infty). \tag{3.10}$$

Using (3.8) and (3.9), from (3.5), we obtain the following expression for the coordinate of the temperature jump in the water filtration zone:

$$n = 0\colon \quad \zeta_{(T)} = \frac{P_e - P_{(s)}}{2(\text{Ja}_{(T)} + 1)}\frac{1}{\zeta_{(s)}}, \qquad n = 1\colon \quad \zeta_{(T)}^2 = \frac{\tilde q}{2(\text{Ja}_{(T)} + 1)}. \tag{3.11}$$

From (3.6) and (3.7), using (3.8) and (3.9), we obtain the system for the self-similar coordinate of the phase-transition boundary and the dimensionless pressure on this boundary:

$$n = 0\colon \qquad P_e - P_{(s)} = 2(\text{Ja}_{(s)} + 1)\zeta_{(s)}^2,$$

$$\rho_{(s)}(P_{(s)} - 1)\exp\Big(-\frac{\zeta_{(s)}^2}{\tilde\eta}\Big)\Big/\int_{\zeta_{(s)}}^\infty \exp\Big(-\frac{\zeta^2}{\tilde\eta}\Big)d\zeta = 2\tilde\mu(\tilde\rho_{(s)} + \text{Ja}_{(s)})\zeta_{(s)};$$

$$n = 1\colon \qquad \tilde q = 2(\text{Ja}_{(s)} + 1)\zeta_{(s)}^2, \tag{3.12}$$

$$\tilde\rho_{(s)}(P_{(s)} - 1)\zeta_{(s)}^{-1}\exp\Big(-\frac{\zeta_{(s)}^2}{\tilde\eta}\Big)\Big/\int_{\zeta_{(s)}}^\infty \zeta^{-1}\exp\Big(-\frac{\zeta^2}{\tilde\eta}\Big)d\zeta = 2\tilde\mu(\tilde\rho_{(s)} + \text{Ja}_{(s)})\zeta_{(s)}.$$

For the coordinate of the labelled boundary in the vapor filtration region, we have

$$(P_{(s)} - 1)\zeta_{(m)}^{-n}\exp\Big(-\frac{\zeta_{(m)}^2}{\tilde\eta}\Big)\Big/\int_{\zeta_{(s)}}^\infty \zeta^{-n}\exp\Big(-\frac{\zeta^2}{\tilde\eta}\Big)d\zeta = 2\zeta_{(m)}. \tag{3.13}$$

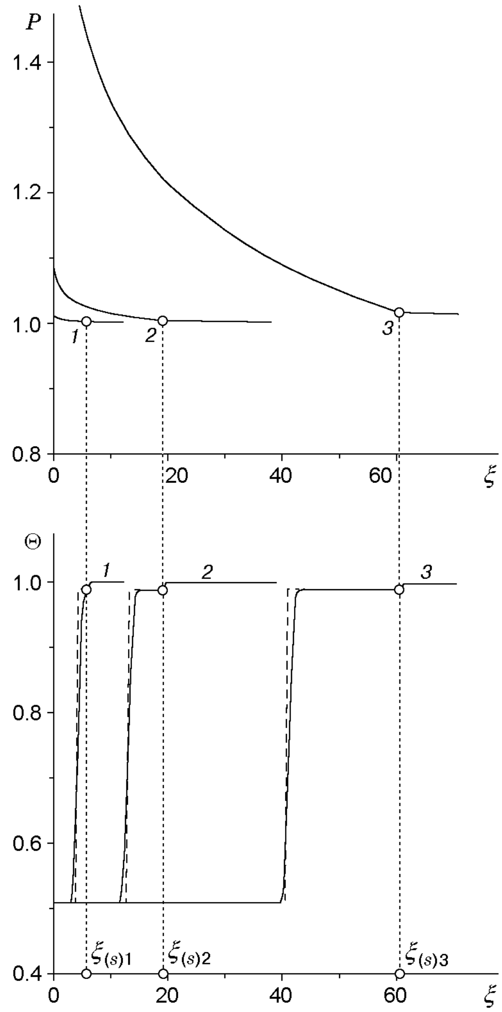

Fig. 4. Comparison of the analytical solutions of Eqs. (2.2) and (2.5) (solid curves) and the solutions of the equations with temperature jumps (3.9) and (3.10) (dashed curves) for $q = 10^{-4}$ (1), 10^{-3} (2), and 10^{-2} m^2/sec (3).

Figure 4 compares the analytical solutions of (2.2) and (2.5) (solid curves) and the solutions with temperature jumps (3.9) and (3.10) (dashed curves) obtained for $p_0 = 10^7$ Pa, $T_0 = 590$ K, $T_e = 300$ K, $k = 10^{-12}$ m^2, and $m = 0.2$. Curves 1–3 correspond to the flow rates of injected water $q = 10^{-4}$, 10^{-3}, 10^{-2} m^2/sec, respectively. It is obvious that the pressure distributions practically coincide. In this case, for the coordinate of the labelled boundary determined from Eq. (2.7), we obtained values $\xi_{(m)} = 8.53$, 26.6, and 81.2, and for the coordinate $\xi_{(m)}$ determined from Eq. (3.13), values $\xi_{(m)} = 8.81$, 25.6, and 78.1. Thus, the solution with temperature jumps describes satisfactorily the evolution of the pressure and temperature fields in the case of rather large permeabilities of the porous medium and the high flow rates of injected water. It should be noted that the self-similar coordinate ζ used in the solution with temperature jumps is related to the self-similar coordinate ξ as follows: $\xi = \zeta\sqrt{æ_{\text{liq}}/a}$.

For the case $p_0 = 10^6$ Pa, $T_0 = 590$ K, and $k = 10^{-12}$ m^2, Fig. 5 shows curves of the self-similar coordinates of the phase-transition boundary $\xi_{(s)}$ and the labelled boundary $\xi_{(m)}$, and the pressure $P_{(s)}$ versus the water injection rate q. The dashed curves are obtained from Eqs. (2.6) using the solution of the heat-conduction equation and the solid curves are obtained from Eqs. (3.12) using the approximate solutions with a temperature jump. The dot-and-dashed curve corresponds to the coordinate of the temperature jump $\xi_{(T)}$ in the water filtration region obtained from Eq. (3.11). From Fig. 5 it follows that with increase in the flow rate q of injected water, the pressures on the phase-transition boundary are close. In this case, the self-similar coordinates of the phase transitions practically coincide.

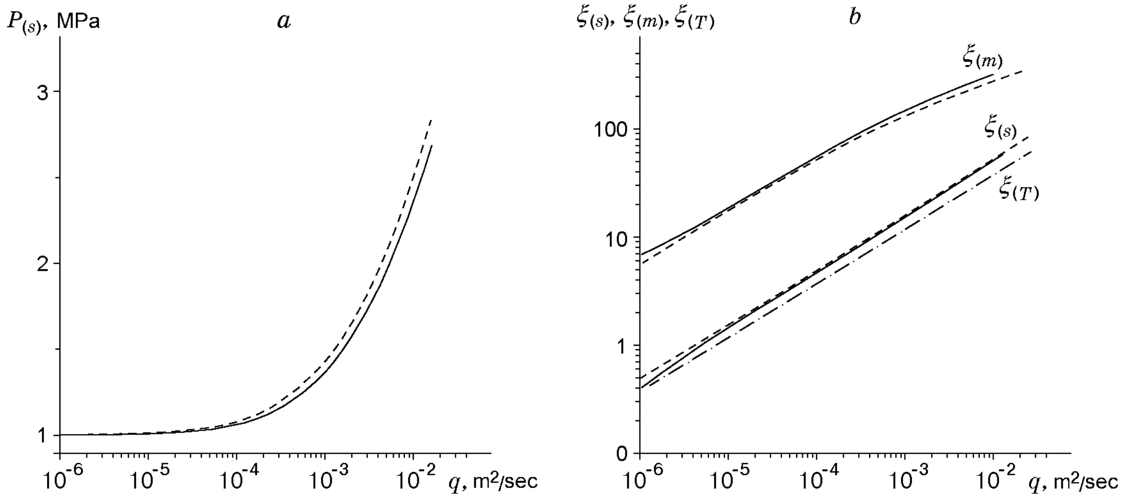

Fig. 5. Pressure $P_{(s)}$ on the phase-transition boundary (a) and the self-similar coordinates of the phase-transition boundary $\xi_{(s)}$ and the labelled boundary $\xi_{(m)}$ (b) versus the injection rate q, obtained from Eqs. (2.6) (dashed curves) and approximate solutions of the equations with temperature jumps (3.12) (solid curves).

Conclusions. An analysis of the solution of the problem of water injection into a geothermal reservoir saturated with vapor shows that in most cases of practical interest, injection occurs in the convective heat transfer regime in the water filtration and vaporization region on the phase-transition boundary. The filtration regime with a pressure "well" can occur only at very low rates of water injection and for anomalously low permeability. In addition, this regime can be observed when the initial state of the vapor is close to the state of saturation.

In the cases of water injection into a porous medium of practical interest there is a step-function temperature distribution. With allowance for this, a rather simple analytical solution with two temperature jumps describing water injection was constructed.

REFERENCES

1. M. J. O'Sullivan, "Geothermal reservoir simulation," *Int. J. Energ. Res.*, **9**, No. 3, 319–332 (1985).
2. K. Pruess, C. Calore, R. Celati, and Y. S. Wu, "An analytical solution for heat transfer at the boiling front moving through a porous medium," *Int. J. Heat Mass Transfer*, **30**, No. 12, 2595–2602 (1987).
3. S. K. Garg and J. W. Pritchett, "Cold water injection into single- and two-phase geothermal reservoirs," *Water Resour. Res.*, **26**, No. 2, 331–338 (1990).
4. K. Pruess, "Grid orientation and capillary pressure effects in the simulation of water injection into depleted vapor zones," *Geothermics*, **20**, Nos. 5/6, 257–277 (1991).
5. V. R. Syrtlanov and V. Sh. Shagapov, "Filtration of a boiling liquid in a porous medium," *Teplofiz. Vysok. Temp.*, **32**, No. 1, 87–93 (1994).
6. A. A. Barmin and G. G. Tsypkin, "Two-front mathematical model of water injection into a geothermal reservoir saturated with vapor," *Izv. Ross. Akad. Nauk, Mekh. Zhidk. Gaza*, No. 3, 105–112 (2000).
7. V. Shagapov, L. A. Nasyrova, and É. V. Galiakbarova, "Water injection into a porous medium saturated with vapor," *Teplofiz. Vysok. Temp.*, **38**, No. 5, 811–818 (2000).